

Determination of the momentum distribution of nucleons in ${}^3\text{He}$ and ${}^3\text{H}$ nuclei from the data for the reactions ${}^3\text{He}p \rightarrow ppd$ and ${}^3\text{H}p \rightarrow pnd$

S. K. Abdullin, A. V. Blinov, I. A. Vanyushin, V. E. Grechko, S. M. Zombkovskii, Yu. V. Korolev, Ya. M. Selektor, V. V. Solov'ev, V. F. Turov, I. V. Chuvilo, and V. N. Shulyachenko
Institute of Theoretical and Experimental Physics

(Submitted 13 March 1989)

Pis'ma Zh. Eksp. Teor. Fiz. **49**, No. 8, 413–417 (25 April 1989)

The momentum distribution of nucleons in ${}^3\text{He}$ and ${}^3\text{H}$ nuclei at the spectator-deuteron momenta of $q < 0.3 \text{ GeV}/c$ has been determined from the data on the reactions $p({}^3\text{He}, pp)d$ and $p({}^3\text{H}, pn)d$. The experimental data were obtained in the ITEP 80-cm liquid-hydrogen bubble chamber which was exposed to separated beams of $5\text{-GeV}/c$ ${}^3\text{He}$ and ${}^3\text{H}$ nuclei. The pole-dominance criteria have been analyzed.

One of the most important characteristics of ${}^3\text{He}$ and ${}^3\text{H}$ nuclei is the nuclear vertex function (NVF), which is defined as the integral for the overlap of the wave functions of the nucleus and the spectator nuclear fragments (the d or NN pairs).

In our previous studies^{1,2} we have obtained the nuclear vertex functions of the decays ${}^3\text{He} \rightarrow pd$ and ${}^3\text{He} \rightarrow ppn$ from the reactions ${}^3\text{He}p \rightarrow ppd$ and ${}^3\text{He}p \rightarrow 3pn$ at the ${}^3\text{He}$ momenta of 2.5 and 5 GeV/c . Special effort was made to carefully select the events involving quasielastic pN scattering which correspond to the diagrams in Fig. 1a (to extract the NVF of the total decay, we used the diagram in Fig. 1a, in which the deuteron was replaced by a spectator pN pair). We tested all the dominance criteria of the pole approximation which were formulated in Ref. 3, in particular, the Treiman-Yang criterion which is very sensitive to the effects produced by mechanisms other than the pole mechanism. Such a detailed analysis has heretofore not been carried out (such an analysis is possible only when the momenta of all the secondary particles are known).

In this study (first) we investigated the nuclear vertex functions of the decay ${}^3\text{He} \rightarrow pd$ in the momentum range of the spectator deuterons $0.16 < q < 0.3 \text{ GeV}/c$ (in Ref. 1 the constraint $q < 0.16 \text{ GeV}/c$ was imposed) and (second) we obtained new data on the nuclear vertex functions of the decay ${}^3\text{H} \rightarrow nd$ at $q < 0.3 \text{ GeV}/c$ from the reaction ${}^3\text{H}p \rightarrow pnd$.

The experimental data were obtained in the ITEP 80-cm liquid-hydrogen bubble chamber which was exposed to separated beams of $5\text{-GeV}/c$ ${}^3\text{He}$ and ${}^3\text{H}$. We selected 5583 events of the reaction

$${}^3\text{He}p \rightarrow ppd, \tag{1}$$

and 10 059 events of the reaction

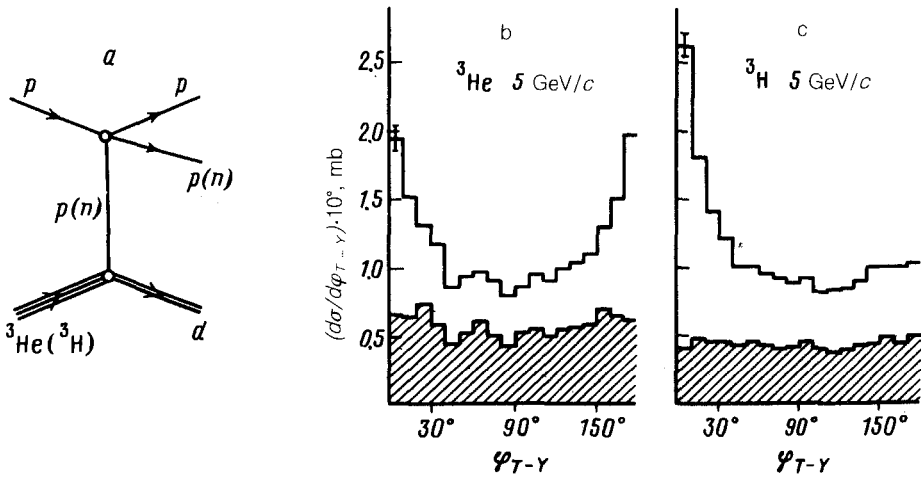


FIG. 1. (a) Diagram of quasielastic pN scattering; (b) and (c) distributions over the Treiman-Yang angle (see the text proper) for the events in the ${}^3\text{He}p \rightarrow ppd$ and ${}^3\text{H}p \rightarrow pnd$ reactions, respectively. The unshatched histograms correspond to the total number of the reaction events with two restrictions indicated in the text proper.

$${}^3\text{H}p \rightarrow pnd. \tag{2}$$

The cross sections of reactions (1) and (2) were found to be 20.6 ± 0.3 and 20.4 ± 0.2 , respectively (the errors are statistical; the systematic error in the absolute normalization of the cross sections was 5%).

The procedure used to extract the nuclear vertex functions from the experimental data was described in detail in our previous studies.^{1,2} We will establish here only the relationship between the momentum distribution of $\rho_2(q)$ and the differential cross sections of reactions (1) and (2):

$$\rho_2(q) = \frac{8m\pi^2 \lambda(s, m^2, m_3^2_{\text{He}({}^3\text{H})})}{m_{3\text{He}({}^3\text{H})}^2 \Phi(t)} \frac{d\sigma}{dq^2}, \tag{3}$$

$$\Phi(t) = \frac{s_+(t)}{\max[s_-(t), 4m^2]} ds_1 \sigma_{el}^{pN}(s_1, t) \lambda^{1/2}(s_1, m^2, m^2), \tag{4}$$

where m is the nucleon mass, $\lambda(x, y, z) = (x + y + z)^2 - 4yz$, q is the deuteron momentum, s and s_1 are the square invariant masses of the pNd and pN systems, t is the square of the 4-momentum transfer from the three-particle nucleus to a deuteron, and $\sigma_{el}^{pN}(s_1, t)$ is the off-shell elastic pN scattering cross section. Such a simple relation between $\rho_2(q)$ and $d\sigma/dq^2$ naturally exists only in a pole approximation.

Two restrictions were imposed on the selection of the events corresponding to the quasielastic-scattering diagram in Fig. 1a: 1) $q < 0.3$ GeV/c and 2) $|\cos \theta^*| < 0.8$, where θ^* is the scattering angle between the primary and secondary protons in the

c.m. frame of the pp or pn pair. The use of these selection criteria left us for the subsequent analysis with 2548 events from reaction (1) and 3832 events from reaction (2). The first restriction was imposed to accurately identify that component of the diagram which involves the deuteron exchange (the pn pair), while the second restriction allows us to exclude to a considerable degree that region of the phase space in which the final-state interaction is appreciable.⁴

The imposition of these two restrictions shows that 1) the distribution in the Treiman-Yang angle, φ_{T-Y} , in Fig. 1, b and c, is essentially isotropic (φ_{T-Y} is the angle between the planes formed by the momentum of the three-particle nucleus and the momentum of the deuteron, on the one hand, and by the momenta of the secondary nucleons, on the other; all of the momenta are given in the rest frame of the initial proton); 2) the nuclear vertex functions do not depend on the initial energy (see Fig. 2); 3) the number of events with a relative kinetic energy of the Nd system lower than 80 MeV (i.e., an energy at which a strong final-state interaction is expected to occur) is no greater than 15%; 4) the number of events with a noncoplanar angle greater than 4° does not exceed 10%; 5) the average momentum transfer from the initial proton to the fastest secondary proton is ~ 0.7 GeV/ c in reaction (1) and ~ 0.9 GeV/ c in reaction (2) (i.e., these momenta are much larger than the inverse nuclear radius, which is ~ 0.1 GeV/ c); 6) if we gradually introduce more rigorous restrictions which account for the exclusion of the final-state-interaction events ($|\cos \theta^*| < 0.6$ and $|\cos \theta^*| < 0.4$), the nuclear vertex functions remain constant within the experimental errors (the characteristics of the suppression of the final-state interaction, 3)–5), in this case improve considerably). Accordingly, results 1)–5) show that the criteria used to select the quasielastic-scattering events are correct.

The elastic cross sections of the pp and pn scattering, which are used to determine the nuclear vertex functions from the data on reactions (1) and (2), were parametrized on the mass shell. Both the results of the phase analysis and the compilation of the differential cross sections were used in this case. At the kinetic energy lower than 0.8 GeV the experimental data on the elastic pp and pn cross sections in the range of $|\cos \theta^*| < 0.8$ under consideration are in agreement with each other and are in excellent agreement with the results of the phase analysis.^{5,6} But at kinetic energies ~ 1 GeV, there is a discrepancy in the experimental data and in the results of the phase analysis, which accounts for a $\sim 5\%$ uncertainty in the values of the nuclear vertex functions (this uncertainty lies within the limits of the statistical errors). We have studied¹ on the basis of the Mongan⁷ model the role played by the off-shell effects by extracting the nuclear vertex functions from reaction (1) at 2.5 GeV/ c of ^3He nuclei (i.e., at a kinetic energy of 0.318 GeV, which is essentially the applicability limit of the model). We found that at $q < 0.16$ GeV/ c the off-shell effects increase the values of the nuclear vertex function by less than 1%.

Our final results for the momentum distributions, $\rho_2(q)$, of nucleons in the ^3He and ^3H nuclei are shown in Fig. 2, a and b (the errors are statistical). Also shown in this figure are the results of other studies and our calculations in the potential model with three potentials: (a) with the Reid potential (the dotted curve taken from Refs. 1, 2, and 4; the S and D components of the vertex functions of ^3H and d in this case were taken into account; the parametrizations of the vertex functions of ^3H and d were

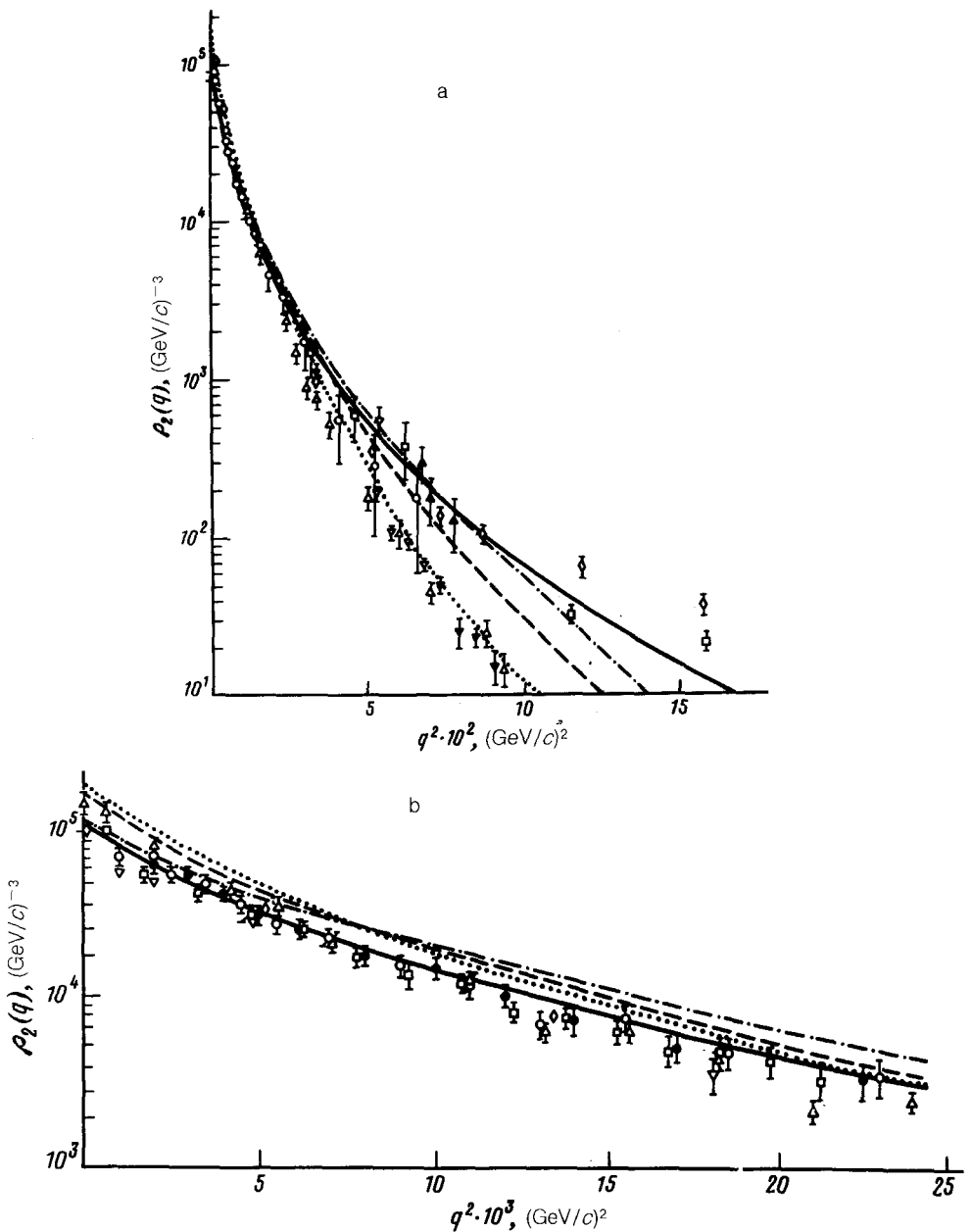


FIG. 2. (a) Momentum distribution of nucleons in ${}^3\text{He}$ and ${}^3\text{H}$ nuclei \circ and \bullet —our data from the reaction $p({}^3\text{He}, 2p)d$, respectively, at $T_p = 0.318$ and 978 GeV; \blacksquare —our data from the reaction $p({}^3\text{H}, pn)d$ at $T_p = 0.978$ GeV; ∇ —SREL data¹⁴ from the reaction ${}^3\text{He}(p, pd)d$ at $T_p = 0.59$ GeV; \blacktriangle —TRIUMF data from the reaction ${}^3\text{He}(p, pd)p$ and \square —from the reaction ${}^3\text{He}(p, 2p)d$ at $T_p = 0.45$ GeV (Ref. 15); \triangle —Saclay data from the reaction ${}^3\text{He}(e, e'p)d$ at $T_e = 0.53$ GeV (Ref. 16); ∇ —NIKHEF data from the same reaction at $T_e = 0.39$ GeV (Ref. 17). The solid, dot-dashed, dotted, and dashed curves are calculations for the Yamaguchi, Mongan, RSC, and QCB potentials, respectively (see the text proper); (b) the same data as in Fig. 2a, but only for the region $q < 16$ GeV/c and on the q -expanded scale.

taken from Refs. 8 and 9, respectively; the NVF for the Paris potential and the RSC potential are nearly identical¹⁰; (b) with a separable Mongan⁷ potential of second rank (the dot-dashed curve; only the *S* components of the vertex functions of ³H and *d* were taken into account, the *D* components of this potential are small; the parametrization of the vertex function of ³H and *d* were taken from Refs. 11 and 7, respectively; (c) with the separable Yamaguchi potential (the solid curve; the VF of ³H was taken from Ref. 12, and the vertex function of the deuteron for the RSC potential was taken from Ref. 9). The dashed curve in Fig. 2 shows the results of a calculation¹³ with a potential in the model of the composite quark bags (the *S* and *D* components of the VF of ³H and *d* were taken into account).

We see in Fig. 2 that the proton momentum distributions in the ³He nucleus and the neutron momentum distribution in the ³H nucleus are in good agreement with each other within error limits (the Coulomb corrections are small¹) and at $q < 0.2$ GeV/*c* they also agree well with the results of the studies of SREL,¹⁴ TRIUMF,¹⁵ and Saclay¹⁶ (after the authors renormalized their earlier data by $\sim 20\%$). To obtain the values of ρ_2 which were reported in Refs. 14–16, the values in Fig. 2, a and b, should be divided by $(2\pi)^3$. Among the theoretical curves calculated with realistic potentials, the curve that comes closest, on the whole, to our data is the curve for the composite quark bags. The dependence $\rho_2(q)$ obtained by us can be approximated well by a function of the type $A_1 \exp(-b_1 q^2) + A_2 \exp(-b_2 q^2)$ with the parameters $A_1 = 7.86 \pm 0.59 \times 10^4$ (GeV/*c*)⁻³, $b_1 = 2.63 \pm 0.31 \times 10^2$ (GeV/*c*)⁻², $A_2 = 1.39 \pm 0.42 \times 10^4$ (GeV/*c*)⁻³, $b_2 = 6.92 \pm 0.90 \times 10^1$ (GeV/*c*)⁻² for $\chi^2/DF = 0.46$.

It is our pleasant duty to thank Y. S. Kalashnikov, I. M. Narodetskiĭ, and Yu. A. Simonov for useful discussions.

- ¹A. V. Blinov *et al.*, Preprint ITEF-40, 1984, p. 21; Phys. G: Nucl. Phys. **11**, 623 (1985).
²A. V. Blinov *et al.*, Yad. Fiz. **45**, 619 (1987) [Sov. J. Nucl. Phys. **45**, 387 (1987)]; Nucl. Phys. A **469**, 566 (1987).
³V. M. Kolybasov, G. A. Leksin, and I. S. Shapiro, Usp. Fiz. Nauk **113**, 299 (1974) (*sic*).
⁴A. V. Blinov *et al.*, Yad. Fiz. **41**, 1440 (1985) [Sov. J. Nucl. Phys. **41**, 913 (1985)]; Nucl. Phys. A **451**, 701 (1986).
⁵R. A. Arndt *et al.*, Phys. Rev. D **28**, 97 (1983).
⁶R. Dubois, Nucl. Phys. A **377**, 554 (1982).
⁷T. R. Mongan, Phys. Rev. **178**, 1597 (1964).
⁸Ch. Hajduk, A. M. Green, and M. E. Sainio, Nucl. Phys. A **337**, 13 (1980).
⁹P. Bosted and J. M. Laget, Nucl. Phys. A **296**, 413 (1978).
¹⁰H. Meier-Hajduk, CH. Hajduk *et al.*, Nucl. Phys. A **395**, 332 (1983).
¹¹V. V. Kotlyar and A. V. Shebeko, Preprint KhFTI-84-26, Moscow, 1984, p. 20.
¹²I. A. Vanyushin *et al.*, Yad. Fiz. **35**, 90 (1982) [Sov. J. Nucl. Phys. **35**, 52 (1982)]; Nucl. Phys. A **377**, 585 (1982).
¹³Yu. S. Kalashnikova, I. M. Narodetskiĭ, and V. P. Yurov, Preprint ITEF-73-88, Moscow, 1988, p. 29.
¹⁴P. Kitching *et al.*, Phys. Rev. C **6**, 769 (1972).
¹⁵E. Epstein *et al.*, Phys. Rev. C **32**, 967 (1985).
¹⁶E. Jans *et al.*, Nucl. Phys. A **475**, 687 (1987).
¹⁷P. H. M. Keizer *et al.*, Phys. Lett. B **197**, 29 (1987).

Translated by S. J. Amoretti